Elucidation of a Monovalent Cation Dependence and Characterization of the Divalent Cation Binding Site of the Fosfomycin Resistance Protein (FosA)†

Bryan A. Bernat, L. Timothy Laughlin, and Richard N. Armstrong*

Departments of Biochemistry and Chemistry and Center in Molecular Toxicology, Vanderbilt University School of Medicine, Nashville, Tennessee 37232-0146

Received February 18, 1999; Revised Manuscript Received April 8, 1999

ABSTRACT: The fosfomycin resistance protein FosA is a member of a distinct superfamily of metalloenzymes containing glyoxalase I, extradiol dioxygenases, and methylmalonyl-CoA epimerase. The dimeric enzyme, with the aid of a single mononuclear Mn^{2+} site in each subunit, catalyzes the addition of glutathione (GSH) to the oxirane ring of the antibiotic, rendering it inactive. Sequence alignments suggest that the metal binding site of FosA is composed of three residues: H7, H67, and E113. The single mutants H7A, H67A, and E113A as well as the more conservative mutants H7Q, H67Q, and E113Q exhibit marked decreases in the ability to bind Mn^{2+} and, in most instances, decreases in catalytic efficiency and the ability to confer resistance to the antibiotic. The enzyme also requires the monovalent cation K^+ for optimal activity. The K^+ ion activates the enzyme 100-fold with an activation constant of 6 mM, well below the physiologic concentration of K^+ in *E. coli*. K^+ can be replaced by other monovalent cations of similar ionic radii. Several lines of evidence suggest that the K^+ ion interacts directly with the active site. Interaction of the enzyme with K^+ is found to be dependent on the presence of the substrate fosfomycin. Moreover, the E113Q mutant exhibits a k_{cat} which is 40% that of wild-type in the absence of K^+. This mutant is not activated by monovalent cations. The behavior of the E113Q mutant is consistent with the proposition that the K^+ ion helps balance the charge at the metal center, further lowering the activation barrier for addition of the anionic nucleophile. The fully activated, native enzyme provides a rate acceleration of $>10^{15}$ with respect to the spontaneous addition of GSH to the oxirane.

FosA is a manganese metalloenzyme known to confer resistance to the broad-spectrum antibiotic fosfomycin, (*1R,2S*)-epoxypropylphosphonic acid (*1*−*3*). The enzyme, with participation of the divalent cation Mn^{2+}, catalyzes the addition of glutathione (GSH)[1] at carbon-1 of the antibiotic to give the biologically inactive adduct shown in Scheme 1. FosA is a member of a superfamily of metalloenzymes that includes glyoxalase I, the extradiol dioxygenases, and methylmalonyl-CoA epimerase (*2*, *4*). Pairwise sequence alignments guided by the crystal structures of human glyoxalase I (*5*) and bacterial meta-cleaving dioxygenases (*6*) suggest that the ligand environment about the metal in FosA includes the side chains of H7 and E113 as illustrated in Scheme 2. Although experimental evidence for the involvement of these residues in either metal ion binding or catalysis is lacking, electron paramagnetic resonance spectroscopy suggests that three of the metal coordination sites

Scheme 1

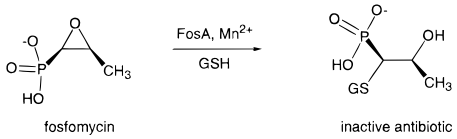

Scheme 2

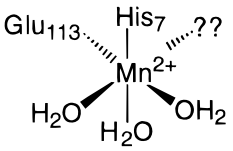

in the E·Mn^{2+} complex are occupied by water molecules (*2*). The sixth ligand completing the octahedral metal site has not been identified.

The exact role of the metal ion in catalysis is unclear. The profound changes seen in the EPR spectrum of enzyme-bound manganese upon the binding of fosfomycin suggest that the substrate may coordinate to the metal center, displacing one or more of the water ligands (*2*). Fosfomycin is very stable with respect to nucleophilic substitution. Therefore, this hypothesis is attractive in that it is easy to envision a role for the metal in neutralizing the charge on the phosphonate or providing electrophilic assistance by coordination with the oxirane oxygen. No other metals or cofactors have been reported to be involved in catalysis. Since the rate constant for the spontaneous addition of GSH

† Supported by National Institutes of Health Grants R01 AI42756, P30 ES00267, and T32 ES07028. L.T.L. was a recipient of National Research Service Award F32 GM18296 from the National Institute of General Medical Sciences.

* Address correspondence to this author. Phone: 615 343-2920. FAX: 615 343-2921. Email: r.armstrong@vanderbilt.edu.

[1] Abbreviations: GSH, glutathione; fos, fosfomycin; Tris, tris-(hydroxymethyl)aminomethane; MES, 2-(*N*-morpholino)ethanesulfonic acid; AQC, 6-aminoquinolyl-*N*-hydroxysuccinimidyl carbamate; IPTG, isopropyl β-D-thiogalactoside; DTT, dithiothreitol; TCA, trichloroacetic acid; EDTA, ethylenediaminetetraacetic acid; EPR, electron paramagnetic resonance; NMR, nuclear magnetic resonance; HPLC, high-performance liquid chromatography; PRR, proton relaxation rate.

10.1021/bi990391y CCC: $18.00
Published on Web 05/14/1999

to fosfomycin has not been reported, there is no reliable estimate of the rate acceleration provided by the enzyme.

In this paper we provide experimental evidence that the protein ligands involved in the divalent cation binding site are H7, H67, and E113. The single mutants H7A, H67A, and E113A as well as the more conservative mutants H7Q, H67Q, and E113Q exhibit marked decreases in the ability to bind Mn^{2+} and, in most instances, decreases in catalytic efficiency and the ability to confer resistance to the antibiotic. In addition, evidence is presented that the enzyme also requires the monovalent cation K^+ for optimal activity. Interaction of the enzyme with K^+ is found to be dependent on the presence of the substrate, fosfomycin. Moreover, the E113Q mutant exhibits a k_{cat} which is 40% that of wild-type and independent of K^+, suggesting that the activation by monovalent cations involves neutralization of the carboxylate of E113. The fully activated, native enzyme provides a rate acceleration of $>10^{15}$ with respect to the spontaneous addition of GSH to the oxirane.

EXPERIMENTAL PROCEDURES

Materials. Fosfomycin disodium salt, 2-(*N*-morpholino)-ethanesulfonic acid (MES), and 4-(2-hydroxyethyl)piperazine-1-ethanesulfonic acid (HEPES) were purchased from Fluka (Ronkonkoma, NY). Tris(hydroxymethyl)aminomethane hydrochloride (Tris), tetrabutylammonium (TBA) chloride, TBA hydroxide, manganese acetate, LiCl, RbCl, and GSH were obtained from Sigma (St. Louis, MO). Tetramethylammonium (TMA) chloride and TMA hydroxide were purchased from Aldrich (Milwaukee, WI). KCl and NH_4Cl were purchased from Mallinckrodt (Paris, KY). 6-Aminoquinolyl-*N*-hydroxysuccinimidyl carbamate (AQC) was purchased from Waters (Milford, MA). $MnCl_2$ was of Puratronic grade and purchased from Alfa Inorganics (Ward Hill, MA). CsCl was obtained from Pharmacia (Uppsala, Sweden). *Escherichia coli* strains BL-21(DE3) and BL-21(DE3)pLysS were purchased from Novagen (Madison, WI).

Nonenzymatic Reaction of GSH and Fosfomycin. Small-scale reactions used for rate determinations ($\pm$5 mM Mg^{2+}) contained 250 mM GSH (pH adjusted to 8.0 with TMA-OH for the sample without Mg^{2+} and KOH for the sample with Mg^{2+}), 250 mM fosfomycin (TMA salt), 2 units/mL GSH reductase, 1 mM NADPH, 100 mM HEPES/TMA-OH (pH 8.0) for the sample without Mg^{2+}, and 100 mM HEPES/KOH (pH 8.0) for the sample with Mg^{2+}, in 1 mL, and were incubated in the dark at 25 °C for 5 days. Aliquots were removed daily and derivatized with the AQC-tag reagent and analyzed by HPLC to follow the reaction and decomposition of substrates. FosA was also added to a portion of these aliquots to confirm the integrity of fosfomycin by comparing the product peak areas as the reaction progressed. The formation of GS−fosfomycin product was linear for 3 days. HPLC analysis of the derivatized reactions showed the GSH peptide began to hydrolyze after that time. The bimolecular rate constant for the spontaneous reaction was estimated from the initial rate using the relationship $k = (d[P]/dt)/[GSH]\cdot[fos]$.

Preparative-scale reactions contained 250 mM GSH, 125 mM fosfomycin disodium salt, 100 mM HEPES/KOH, 0.5 unit/mL GSH reductase, and 1 mM NADPH (pH 8.0) $\pm$ 5 mM $MgCl_2$ in 50 mL and were incubated and analyzed as described above for 2 weeks. Samples were then loaded onto an AG1-X2 column and purified as described previously (*3*) except a 500 mL gradient (0−500 mM) of NH_4HCO_3 was used. Ten milligrams of purified material was resuspended in 500 μL of D_2O for NMR analysis. The products were fully characterized by ^1H, ^{13}C, ^{31}P, and heteronuclear multiple-bond correlation (HMBC) NMR spectroscopy. The HMBC spectrum of the product mixture is given in the Supporting Information. The NMR properties of isomer-1 produced in the enzyme-catalyzed reaction have been previously reported (*3*). *Product Isomer 1*,[2] (*1R,2S*)-1-(*S*-glutathionyl)-2-hydroxypropylphosphonate: ^1H NMR (400.135 MHz, D_2O, pD 2.4) δ 1.32 (d, 3H, J = 6.3 Hz, CHCHC*H*$_3$), 2.13−2.25 (m, 1H, Glu β), 2.48−2.62 (m, 1H, Glu γ), 2.75 (dd, 1H, J = 3.5 and 17.9 Hz, Cys β'), 2.97−3.16 (m, 2H, Cys β, C*H*CHCH$_3$), 3.97−4.02 (m, 2H, Glu α, Gly α), 4.24−4.29 (m, 1H, CHC*H*CH$_3$), 4.54−4.58 (m, 1H, Cys α); ^{13}C NMR (100.614 MHz, D_2O, pD 2.4) δ 20.65 (d, J = 9.6, CHCH*C*H$_3$), 25.71 (s, Glu β), 31.09 (s, Glu γ), 35.26 (d, J = 3.9 Hz, Cys β), 41.37 (s, Gly α), 50.73 (d, J = 137.3 Hz, *C*HCHCH$_3$), 52.80 (s, Glu α), 53.84 (s, Cys α), 67.14 (s, CH*C*HCH$_3$); ^{31}P NMR (161.978 MHz, D_2O, pD 2.4) δ 19.50 (dd, J = 9.3 and 17.1 Hz). *Product Isomer 2*,[2] (*1R,2R*)-2-(*S*-glutathionyl)-1-hydroxypropylphosphonate: ^1H NMR (400.135 MHz, D_2O, pD 2.4) δ 1.40 (d, 3H, J = 7.0 Hz, CHCHC*H*$_3$), 2.13−2.25 (m, 1H, Glu β), 2.48−2.62 (m, 1H, Glu γ), 2.97−3.16 (m, 2H, Cys β, CHC*H*CH$_3$), 3.68 (dd, 1H, J = 6.9 and 9.4 Hz, C*H*CHCH$_3$), 3.97−4.02 (m, 2H, Glu α, Gly α), 4.54−4.58 (m, 1H, Cys α); ^{13}C NMR (100.614 MHz, D_2O, pD 2.4) δ 19.20 (d, J = 5.6 Hz, CHCH*C*H$_3$), 25.71 (s, Glu β), 31.09 (s, Glu γ), 32.01 (s, Cys β), 41.37 (s, Gly α), 44.17 (d, J = 5.4 Hz, CH*C*HCH$_3$), 52.80 (s, Glu α), 53.68 (s, Cys α), 72.41 (d, J = 155.4 Hz, *C*HCHCH$_3$); ^{31}P NMR (161.978 MHz, D_2O, pD 2.4) δ 18.51 (dd, J = 8.3 Hz).

Preparation, Expression, and Purification of Mutant FosA. The Kunkel method (*7*) of mutagenesis was used to create site-directed mutants of the putative FosA metal ligands. Mutants were selected based on the incorporation of a silent mutation which could be tested by restriction digests or the failure to grow in media containing fosfomycin followed by sequencing of the coding region. BL-21(DE3) or BL-21(DE3)pLysS cells (for the H7Q mutant) were transformed with mutant plasmids for expression of protein. All mutants were purified by the published procedure for the native enzyme (*2*). For experiments requiring a nonactivating monovalent cation, the purified enzyme was dialyzed vs 20 mM MES/TMA hydroxide, 1 mM DTT (pH 6.0).

Determination of Minimum Inhibitory Concentration of Fosfomycin. The ability of native and mutant expression plasmids to confer resistance to *Escherichia coli* to fosfomycin was determined using the above transformed BL-21(DE3) or BL-21(DE3)pLysS cells. Aliquots from log phase cultures containing 100 μg/mL ampicillin were added to 7.5 mL cultures containing serial dilutions of fosfomycin and 100 μg/mL ampicillin. Cultures were grown in a shaker at 37 °C without the addition of IPTG or lactose for 6 h. Cell density was determined by taking the absorbance at 600 nm at various times during the growth.

[2] The absolute configuration of isomer 1 has been deduced (*3*). The configuration of isomer 2 has not been determined and is based on the reasonable assumption of inversion of configuration at C-2.

Standard Enzyme Assay and Metal-Ion Activation. A typical assay for wild-type FosA contained 50 nM enzyme, 50 μM $MnCl_2$, 10 mM fosfomycin/TMA, 10 mM GSH, 100 mM KCl, and 100 mM HEPES/TMA hydroxide (pH 8.0) in a total volume of 100 μL. The disodium salt of fosfomycin was converted to the TMA or TBA salt as previously described (*3*). Assays of some mutants contained higher enzyme and metal concentrations. Manganese acetate was used in experiments with thallium acetate as the activating monovalent cation. Samples were incubated at 25 °C for 5 min or less. The HPLC assay was carried out as described previously (*2*) using the AQC reagent (Waters).

Steady-State Kinetics. The k_{cat} and k_{cat}/K_m^{fos} for native FosA were determined with a fixed GSH concentration of 10 mM, varying concentrations of fosfomycin/TMA, 100 mM HEPES/TMA hydroxide (pH 8.0), 50 μM $MnCl_2$, 100 mM KCl, and 1.0 nM enzyme. The assay conditions for mutant enzymes included higher concentrations of enzyme, $MnCl_2$, and 200 mM KCl, except for E113A, which contained 1 M KCl. A correction for the change in fosfomycin concentration during the course of the reaction was applied (*8*) prior to fitting the data to the Michaelis−Menten equation.

EPR Spectroscopy and Water Proton Relaxation Rate Measurements. EPR spectra were recorded at 35 GHz (Q-band) with a Varian E109Q spectrometer in which the temperature of the sample cavity was maintained at 0 °C. EPR spectra at 9 GHz (X-band) were recorded with a Varian E3 spectrometer. The temperature was controlled at 20 °C. The samples were contained in quartz capillary tubes. The binding constant for Mn^{2+} was obtained by scanning the first transition of the typical $g = 2$ sextet. Free and bound Mn^{2+} could be calculated by comparing amplitudes of samples with and without enzyme. The data were fit to a hyperbola to determine a K_d. The longitudinal proton relaxation rate (PRR) of the bulk solvent water was determined with a 180°−τ−90° NMR pulse sequence at 23.4 MHz as described previously (*2*). Dissociation constants (K_d) of fosfomycin from E·Mn^{2+} were determined by fitting the titration data to eq 1 where $1/T_{1p_f}$ is the observed longitudinal water proton relaxation rate in the presence of E·Mn^{2+} and $1/T_{1p_b}$ is the observed longitudinal relaxation rate in the presence of E·Mn^{2+}·S:

$$1/T_{1p} = \frac{\left([E\cdot Mn^{2+}]\frac{1}{T_{1p_f}} + [E\cdot Mn^{2+}\cdot S]\frac{1}{T_{1p_b}}\right)}{[E]_t} \qquad (1)$$

where

$$[E\cdot Mn^{2+}\cdot S] = \frac{b - \sqrt{b^2 - [4([E\cdot Mn^{2+}]_t)([S]_t)]}}{2}$$

$b = K_d + [S]_t + [E\cdot Mn^{2+}]_t$ and $[E\cdot Mn^{2+}] = [E\cdot Mn^{2+}]_t - [E\cdot Mn^{2+}\cdot S]$

RESULTS

Activation of Wild-Type FosA by Monovalent Cations. During the course of determining the steady-state kinetics of FosA, unexpected variations in the initial rates were observed and eventually found to be due to a significant activation of the enzyme by specific monovalent cations. Large cations such as tetramethylammonium (TMA) and tetrabutylammonium do not activate the enzyme and were therefore used as counterions in buffers (100 mM HEPES, pH 8.0) to quantify the activation. The most effective monovalent cation is K^+ which activates FosA ≥100-fold (Table 1) with an activation constant $K_{act}^{K^+} = 6$ mM. Other monovalent cations also activate FosA. Those with atomic radii close to K^+ (Tl^+, NH_4^+, and Rb^+) activate FosA almost as effectively, with K_{act} values of approximately 10 mM. The K_{act} for Tl^+ is actually lower than that for K^+. The activation profile by the various monovalent cations is similar to that seen for pyruvate kinase (*9*, *10*) although the latter enzyme is activated to a much greater extent, about 10^5-fold (*10*).

Table 1: Activation of Wild-Type FosA with Different Monovalent Cations under Standard Assay Conditions

cation	k_{cat} (s^{-1})	$K_{act}^{M^+}$ (mM)	crystal radius (Å)
K^+	600	6.2 ± 1.6	1.33
Tl^+	420	2.4 ± 0.4	1.46
Na^+	60	74 ± 29	0.97
Li^+	50	63 ± 26	0.68
Cs^+	50	86 ± 27	1.67
Rb^+	440	10.4 ± 3.8	1.47
NH_4^+	415	11.9 ± 4.2	1.43

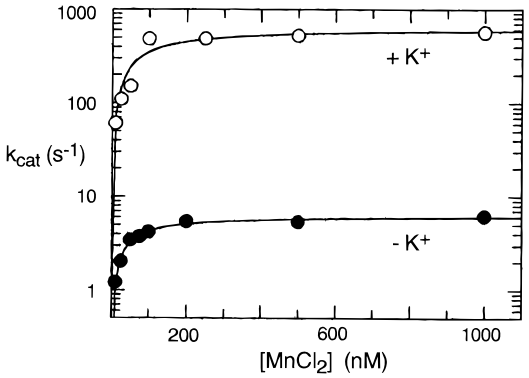

FIGURE 1: Metal ion activation of native FosA by Mn^{2+} in the absence (●) or presence of 100 mM K^+ (○). The solid lines are fits of the data to a hyperbola with $K_{act}^{Mn^{2+}} = 50 \pm 5$ nM and $k_{cat}(app) = 6.1 \pm 0.2$ s^{-1} in the absence of K^+, and $K_{act}^{Mn^{2+}} = 80 \pm 30$ nM and $k_{cat}(app) = 610 \pm 67$ s^{-1} in the presence of K^+.

The activation of the enzyme by monovalent cations does not alter the affinity of the enzyme for Mn^{2+} (data not shown) nor does it significantly alter the K_{act} by Mn^{2+} as illustrated in Figure 1. Furthermore, there is no evidence that monovalent cations interact in any significant way with the binary E·Mn^{2+} complex. For example, there is no difference in the line shape or amplitude of the EPR spectra of E·Mn^{2+} in the presence of 100 mM TMA, K^+, or other monovalent cations. In contrast, K^+ has a pronounced effect on the EPR spectrum of the ternary E·Mn^{2+}·fos complex as shown in Figure 2. In the presence of substrate, K^+ induces a more anisotropic spectrum in which another sextet of transitions appear downfield of the typical $g = 2$ sextet. This spectral signature is similar to that found in the pyruvate kinase·Mn^{2+}·Mg^{2+}·K^+·substrate complexes (*11*, *12*). The same anisotropic spectra of the E·Mn^{2+}·fosfomycin complex were obtained when 15 mM Tl^+ was substituted for K^+ (data not shown). Taken together, these results suggest that the monovalent cation site either is not occupied or has no

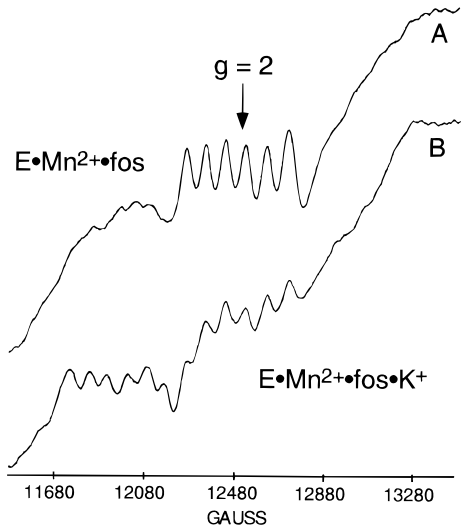

FIGURE 2: EPR spectra (35 GHz) of the E·Mn^{2+}·fos complex in the presence of 100 mM TMA^+ (A) or 100 mM K^+ (B). Both spectra were obtained in the presence of excess enzyme, [E] = 4.6 mM, Mn^{2+} = 3.2 mM, fosfomycin/TMA = 10 mM, in 100 mM HEPES/TMA buffer (pH 8.0).

influence on the coordination sphere of Mn^{2+} in the absence of fosfomycin. In the presence of substrate, monovalent cations clearly alter the coordination environment of the enzyme-bound metal.

The presence of K^+ has a large effect on k_{cat}/K_m^{GSH}. In the presence of saturating (0.5 mM) fosfomycin and 0.1 M K^+ (pH 8.0), the k_{cat}/K_m^{GSH} is $(9.80 \pm 0.76) \times 10^4$ M^{-1} s^{-1}. In the absence of K^+, it is about 50-fold smaller where $k_{cat}/K_m^{GSH} = (1.88 \pm 0.33) \times 10^3$ M^{-1} s^{-1}. The turnover number in the presence of K^+ is $(1.07 \pm 0.03) \times 10^3$ s^{-1} but is difficult to measure accurately in the absence of K^+ due to a large increase in K_m^{GSH} ($\geq$100 mM). Clearly, the presence of K^+ increases the reactivity of the E·Mn^{2+}·fos complex toward the attack of the nucleophile.

Preliminary Identification of Metal Ligands by Sequence Alignment. FosA has been identified as a member of a superfamily of metalloenzymes which include glyoxalase I, manganese- and iron-dependent dioxygenases, and methylmalonyl-CoA epimerase (*2*, *4*). Pairwise sequence alignments generated by a BLAST search (*2*) mapped to the crystal structures of an extradiol dioxygenase (*6*) and human glyoxalase I (*5*) implicate H7 and E113 as metal ligands. The fact that three of the coordination sites of the Mn^{2+} in FosA are occupied by water (*2*) suggests that there is an additional ligand from the protein, not apparent in pairwise alignments, that completes the octahedral geometry of the metal. A more extensive PILEUP multiple sequence alignment of FosA with other fosfomycin resistance proteins from clinical isolates of *Staphylococcus* (*13*) and a genomic sequence from *Bacillus subtilis* (*14*) along with several glyoxalases and methylmalonyl-CoA epimerases clearly suggests that the third protein ligand is H67 (Supporting Information).

Plasmids Encoding FosA with Mutant Divalent Metal Sites. To provide experimental support for the role of the three putative metal ligands in the function of FosA, six plasmids encoding the H7Q, H7A, H67Q, H67A, E113Q, and E113A mutants were prepared. *Escherichia coli* strain BL-21(DE3) is sensitive to as little as 15 μg/mL fosfomycin.

Table 2: Fosfomycin Resistance Conferred by Plasmids Encoding Native and Metal Ligand Mutants of FosA

plasmid or enzyme expressed	MIC fosfomycin[a] (μg/mL)
pET20[b]	15
wild type	15000
H7Q[c]	2500
H7A	120
H67Q	500
H67A	15
E113Q	5000
E113A	60

[a] Resistance determined with transformed BL-21(DE3) cells and expressed as minimum inhibitory concentration (MIC). [b] Control BL-21(DE3) cells transformed with pET20 containing no FosA insert. [c] BL-21(DE3) pLysS cells were used for the H7Q mutant.

Table 3: Dissociation Constants for Mn^{2+} and Activation Constants for Mn^{2+} and K^+ for Wild-Type FosA and Metal Ligand Mutants

enzyme	$K_{act}^{Mn^{2+}}$ [a] (μM)	$K_d^{Mn^{2+}}$ [b] (μM)	K_{act}^{K+} [c] (mM)	fold activation by K^+
wild type	0.08 ± 0.03	<1.5	6.2 ± 1.6	100
H7Q	22 ± 3	105 ± 40	34 ± 8	150
H7A	165 ± 21	125 ± 50	75 ± 20	125
H67Q	1200 ± 200	1500 ± 500	42 ± 5	170
H67A	2200 ± 500	2100 ± 900	48 ± 19	45
E113Q	1.1 ± 0.2	15 ± 5	—[d]	—[d]
E113A	3900 ± 1200	890 ± 280	200 ± 30	16

[a] Determined with standard assay conditions [10 mM fosfomycin/TMA, 10 mM GSH, saturating KCl, 0.1 M HEPES/TMA (pH 8.0)] by varying the Mn^{2+} concentration. [b] Determined by EPR titration of free and bound Mn^{2+}. [c] Determined with standard assay conditions by varying the K^+ concentration. [d] No detectable activation.

When transformed with the wild-type FosA expression plasmid, this same strain is resistant to fosfomycin at concentrations >7.5 mg/mL (*2*), even in the absence of an inducer such as IPTG or lactose. Although most of the mutant plasmids confer some resistance to fosfomycin (Table 2), the resistance is less robust than that conferred by the native expression plasmid. It is also clear from Table 2 that the more conservative glutamine mutants confer superior resistance to the antibiotic. For example, the E113Q mutant confers substantial resistance whereas the H67A mutant appears to be completely ineffective. Interestingly, the H7Q mutant plasmid is toxic to the BL-21(DE3) cells even in the absence of inducer. It was not toxic to the BL-21(DE3)-pLysS strain which exerts tighter control over the promoter. As discussed later, the microbiological properties of the plasmids correlate with the metal binding and catalytic characteristics of the mutant enzymes.

The mutant proteins express as well as the wild type enzyme (200 mg/liter of culture) in the presence of the inducer IPTG. As mentioned above, BL-21(DE3) cells transformed with the H7Q mutant plasmid did not produce colonies. Hence, BL-21 (DE3)pLysS cells were used for production of the H7Q mutant. All the mutants chromatograph similarly to the wild type enzyme. Therefore, the previously reported purification procedure (*2*) was used without modification to obtain the purified mutant enzymes.

Metal Binding and Activation of FosA Mutants. Dissociation and activation constants for Mn^{2+} with the FosA mutants are shown in Table 3. The mutants exhibit increased dissociation constants for Mn^{2+} as illustrated by the examples

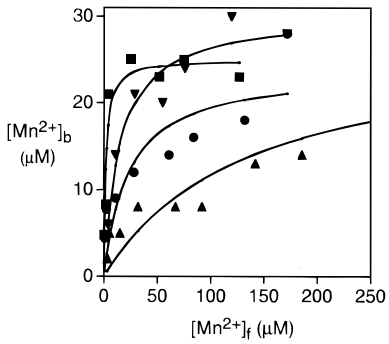

FIGURE 3: Titration of native and mutant FosA with Mn^{2+}. The concentration of subunits in each case was 25 μM. The solid lines represent fits of each experimental data set to a hyperbola with the indicated stoichiometry (n) and dissociation constant ($K_d^{Mn^{2+}}$): native (■), $n = 1.0 \pm 0.06$, $K_d^{Mn^{2+}} = 1.7 \pm 0.7$ μM; E113Q (▼), $n = 1.20 \pm 0.08$, $K_d^{Mn^{2+}} = 15 \pm 4.6$ μM; H7Q (●), $n = 0.96 \pm 0.18$, $K_d^{Mn^{2+}} = 23 \pm 16$ μM; H7A (▲), $n = 1.08 \pm 0.19$, $K_d^{Mn^{2+}} = 140 \pm 60$ μM.

in Figure 3. In general, the effect of replacing each residue with alanine alters the metal binding properties to a greater extent than the more conservative replacement with glutamine which can still act as a ligand to the metal. These results are clearly consistent with the proposition that H7, H67, and E113 function as ligands in the divalent metal ion binding site. The least disruptive mutation, despite the alteration in the charge of the metal site, is E113Q.

The changes in the Mn^{2+} activation constants ($K_{act}^{Mn^{2+}}$) for the mutants roughly parallel the decreased affinity of the enzymes for metal. It is important to note that $K_{act}^{Mn^{2+}}$ need not be equal to $K_d^{Mn^{2+}}$ since the latter is determined in the absence of substrates. In fact, in the wild-type enzyme as well as the more efficient mutants the $K_{act}^{Mn^{2+}}$ is generally lower than the metal dissociation constant, suggesting that the presence of substrates (in particular fosfomycin) may tighten metal binding to the protein.[3]

In addition to altering divalent cation binding, all of the mutations affect, to varying degrees, the activation of the enzyme by K^+ as summarized in Table 3. Mutations of the histidine residues increase the activation constant for K^+ but have little influence on the extent of activation. Perhaps the most interesting observation is that the E113Q mutant is not activated by K^+ and has a k_{cat} that is 40% that of the fully activated native enzyme (Table 4). The removal of the negative charge of the carboxylate seems to result in a preactivated enzyme that is unresponsive to monovalent cations. In addition, the EPR spectrum of the E113Q·Mn^{2+}·fos complex (data not shown), unlike the native complex (Figure 2), is unaffected by the presence of K^+. Although the E113A mutant is activated by K^+, the extent of activation is not nearly as pronounced as in the native enzyme or histidine mutants (Tables 3 and 4), and the activation constant is quite high.

Substrate Binding and Catalytic Characteristics of FosA Mutants. The steady-state kinetic constants for wild-type FosA and the six mutants are listed in Table 4. Some generalizations can be made. In particular, all of the mutants have lower activity and higher $K_{act}^{Mn^{2+}}$ when compared to wild-type FosA. The wild-type enzyme is at least 10 times more efficient than any of the mutants in the presence of K^+. With the exception of H67A, the turnover numbers are substantial in the presence of high concentrations of Mn^{2+}. As expected, the glutamine mutants generally have higher turnover numbers and lower $K_{act}^{Mn^{2+}}$ than the corresponding alanine mutants. One characteristic all of the mutants have in common is a higher K_m for fosfomycin and consequently a lower k_{cat}/K_m^{fos}. However, the E113Q mutant is the least affected with respect to K_m^{fos}. The fact that most of the mutants have respectable turnover numbers but do require higher Mn^{2+} concentrations for full activation is a good indication that the mutations are primarily affecting the metal coordination environment and not other aspects of structure or catalysis.

In several instances the dissociation constant for fosfomycin (K_d^{fos}) can be directly determined by titration of the paramagnetic contribution of Mn^{2+} to the proton relaxation rates (PRR) of water. PRR titrations of the native enzyme done in the presence of 100 mM TMA ($K_d^{fos} = 70$ μM) or K^+ ($K_d^{fos} = 60$ μM) clearly indicate that K^+ does not affect dissociation of the substrate. Moreover, the K_d^{fos} is in good agreement with K_m^{fos} for the native enzyme. In the three instances where titrations could be conducted, the mutants exhibit much higher values for K_d^{fos} (Figure 4) which parallel the increases observed in K_m^{fos} (Table 4).

Rate Acceleration Provided by FosA. To estimate the rate acceleration provided by fully activated FosA, the bimolecular rate constant for the spontaneous addition of GSH to fosfomycin was determined at pH 8 and 25 °C. In the absence of divalent cations, the rate constant for addition was 1.4×10^{-8} M^{-1} s^{-1}. Inclusion of a divalent cation (e.g., 5 mM Mg^{2+}) only marginally enhanced the rate of addition. Therefore, the rate acceleration provided by the enzyme is about 10^{15}. Although the enzyme-catalyzed addition of GSH is regiospecific (*3*), HMBC NMR analysis (Supporting Information) of the spontaneous reaction product indicates that it is a mixture of the two possible regioisomers (Scheme 3). This is somewhat surprising since nucleophilic substitution α to a phosphonate is usually difficult (*15*, *16*). It also contrasts with the HF-catalyzed addition of cysteine to fosfomycin (*17*) and the reaction of the active site cysteine residue of MurA (the biological target of fosfomycin), both of which occur exclusively at carbon-2 (*18*, *19*).

DISCUSSION

Characterization of the Divalent Cation Binding Site. The identity of protein ligands to the metal in the FosA·Mn^{2+} complex suggested in sequence alignments with other members of the same metalloenzyme superfamily is consistent with the physical and functional properties of the mutant enzymes. The mutants alter the metal binding characteristics of the enzyme over a range of $>10^4$ and change the catalytic efficiency over a similar range. Interestingly, there are relatively good correlations between the k_{cat}/K_m^{fos} or $K_d^{Mn^{2+}}$ for the various enzymes and the resistance conferred in *E. coli* by the various plasmids as illustrated in Figure 5. Mutants with $k_{cat}/K_m^{fos} \geq 10^5$ M^{-1} s^{-1} (e.g., H7Q, H67Q, and E113Q) confer considerable resistance while those with $k_{cat}/K_m^{fos} \leq 10^4$ M^{-1} s^{-1} confer marginal to no resistance. It

[3] Evidence from EDTA trapping experiments indicates that fosfomycin decreases the off rate of Mn^{2+} from the protein by a factor of about 10 (B. A. Bernat and R. N. Armstrong, unpublished results).

Table 4: Steady-State Kinetic Parameters for Wild-Type FosA and Metal Ligand Mutants[a]

enzyme	[KCl] (M)	k_{cat} (s^{-1})	k_{cat}/K_m^{fos} (M^{-1} s^{-1})	K_m^{fos} (mM)	K_d^{fos} [b] (mM)
wild type	0.1	658 ± 14	$(1.4 \pm 0.1) \times 10^7$	0.048 ± 0.003	0.062 ± 0.009
wild type	0	5.0 ± 0.3	$(8.6 \pm 1.8) \times 10^5$	0.063 ± 0.01	0.070 ± 0.01
H7Q	0.2	417 ± 19	$(1.4 \pm 0.1) \times 10^5$	4.2 ± 0.4	2.6 ± 0.5[c]
H7A	0.2	67 ± 2	$(1.3 \pm 0.2) \times 10^4$	5.2 ± 0.5	5.6 ± 0.8[c]
H67Q	0.2	720 ± 60	$(1.5 \pm 0.4) \times 10^5$	4.7 ± 0.8	12.0 ± 1.8[c]
H67A	0.2	1.7 ± 0.1	$(4.6 \pm 0.8) \times 10^3$	3.8 ± 0.5	—[d]
E113Q	0.2	265 ± 3	$(5.1 \pm 0.2) \times 10^5$	0.52 ± 0.15	—[d]
E113Q	0	280 ± 8	$(4.0 \pm 0.4) \times 10^5$	0.70 ± 0.09	—[d]
E113A	1.0	150 ± 5	$(1.7 \pm 0.2) \times 10^4$	9.0 ± 0.9	—[d]
E113A	0	15 ± 0.5	$(1.3 \pm 0.2) \times 10^3$	12.0 ± 0.9	—[d]

[a] Determined under standard assay conditions with [GSH] = 10 mM and variable fosfomycin. [b] Determined by PRR titration. [c] Determined in the presence of 60 mM K^+. [d] The change in $1/T_{1p}$ was too small for accurate titration.

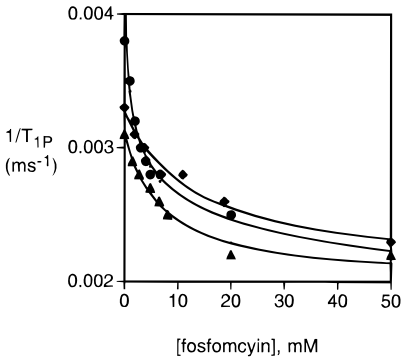

FIGURE 4: Titration of observed water proton relaxation rates ($1/T_{1p}$) of mutant E·Mn^{2+} complexes with fosfomycin. The solid lines are fits of each experimental data set to eq 1 with the indicated values for K_d^{fos}, $1/T_{1p_f}$, and $1/T_{1p_b}$: native (data not shown), $K_d^{fos} = 62 \pm 9$ μM, $1/T_{1p_f} = 23.2 \pm 0.3$ μs^{-1}, and $1/T_{1p_b} = 4.5 \pm 0.3$ μs^{-1}; H7Q (●), $K_d^{fos} = 2.6 \pm 0.5$ mM, $1/T_{1p_f} = 3.84 \pm 0.06$ μs^{-1}, and $1/T_{1p_b} = 2.31 \pm 0.08$ μs^{-1}; H7A (▲), $K_d^{fos} = 5.6 \pm 0.8$ mM, $1/T_{1p_f} = 3.74 \pm 0.03$ μs^{-1}, and $1/T_{1p_b} = 2.05 \pm 0.04$ μs^{-1}; H67Q (◆), $K_d^{fos} = 12.0 \pm 1.8$ mM, $1/T_{1p_f} = 3.24 \pm 0.03$ μs^{-1}, and $1/T_{1p_b} = 2.17 \pm 0.04$ μs^{-1}.

Scheme 3

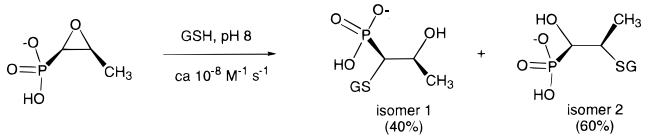

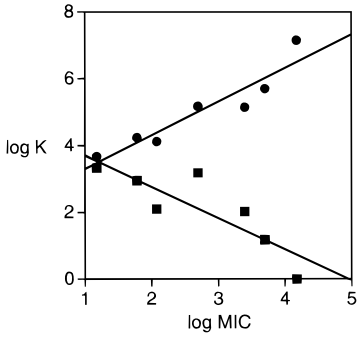

FIGURE 5: Resistance conferred to fosfomycin (log MIC) as a function of $\log(k_{cat}/K_m^{fos})$ (●) and $\log(K_d^{Mn^{2+}})$ (■). The solid lines are linear regression fits to the data with slopes of 1.01 and −0.93 for $\log(k_{cat}/K_m^{fos})$ and $\log(K_d^{Mn^{2+}})$, respectively.

is also clear that the more conservative glutamine mutants are better than their alanine counterparts at binding Mn^{2+} and catalysis. The physical, catalytic, and microbiological data all support the hypothesis that H7, H67, and E113 compose the divalent metal site of FosA. The three solvent-occupied coordination sites are free for ligand replacement in the reaction as described in more detail below.

Catalytic Efficiency of FosA. The catalytic efficiency of FosA is remarkably high considering the very low reactivity of the oxirane ring of fosfomycin. The turnover number with saturating concentrations of both substrates is about 1000 s^{-1}, and the k_{cat}/K_m^{fos} is within a factor of 10 of the generally accepted diffusion limit (10^8 M^{-1} s^{-1}) for enzyme-catalyzed reactions. Although there is no direct evidence that the reaction is diffusion-controlled, it is possible that FosA is an enzyme that has evolved to near its full catalytic potential. In fact, it may be that k_{cat}/K_m^{fos} is limited not by diffusion but by the ligand exchange kinetics in the coordination sphere of the metal.

Role of K^+ in Catalysis. The relatively low $K_{act}^{K^+}$ is far below typical intracellular K^+ concentrations (≥100 mM) in *E. coli* (*20*), suggesting that K^+ is normally involved in the catalytic mechanism and that there is a specific K^+ binding site in the enzyme−substrate complex. Four lines of evidence suggest that the influence of monovalent cations such as K^+ is due to a direct interaction with the active site. The first is the pronounced effect of K^+ on the EPR spectrum of the E·Mn^{2+}·fos complex (Figure 2). The increased anisotropy in the spectrum is a direct indication of a more distorted ligand field about the metal in the presence of K^+. The second indication is that there is no effect of K^+ on the EPR spectrum in the absence of fosfomycin. The third line of evidence is that the activation constant for K^+ is sensitive to alterations in structure of the metal ion binding site (Table 3). Finally, the high basal activity and absence of K^+ activation of the E113Q mutant suggest that the carboxylate of E113 is directly involved in the activation process.

The effect of K^+ appears to be manifest primarily in the transition state for the reaction since k_{cat}, k_{cat}/K_m^{fos}, and k_{cat}/K_m^{GSH} are enhanced by its presence. Although K^+ can be detected spectroscopically in the ground-state E·Mn^{2+}·fos complex (Figure 2), its presence does not affect the dissociation constant (or K_m^{fos}) for this substrate. Even though the addition of K^+ does not alter the stability of the ternary ground-state complex of E·Mn^{2+}·fos in any significant way, it does appear to increase the thermodynamic stability and the reactivity of the quaternary E·Mn^{2+}·fos·GSH complex as suggested by the decrease in K_m^{GSH} and increase in k_{cat}/K_m^{GSH}, respectively.

Possible Catalytic Mechanisms for FosA. There are several mechanistic possibilities for the involvement of monovalent and divalent cations in catalysis. The profound effect of fosfomycin on the EPR spectrum of Mn^{2+} bound to the

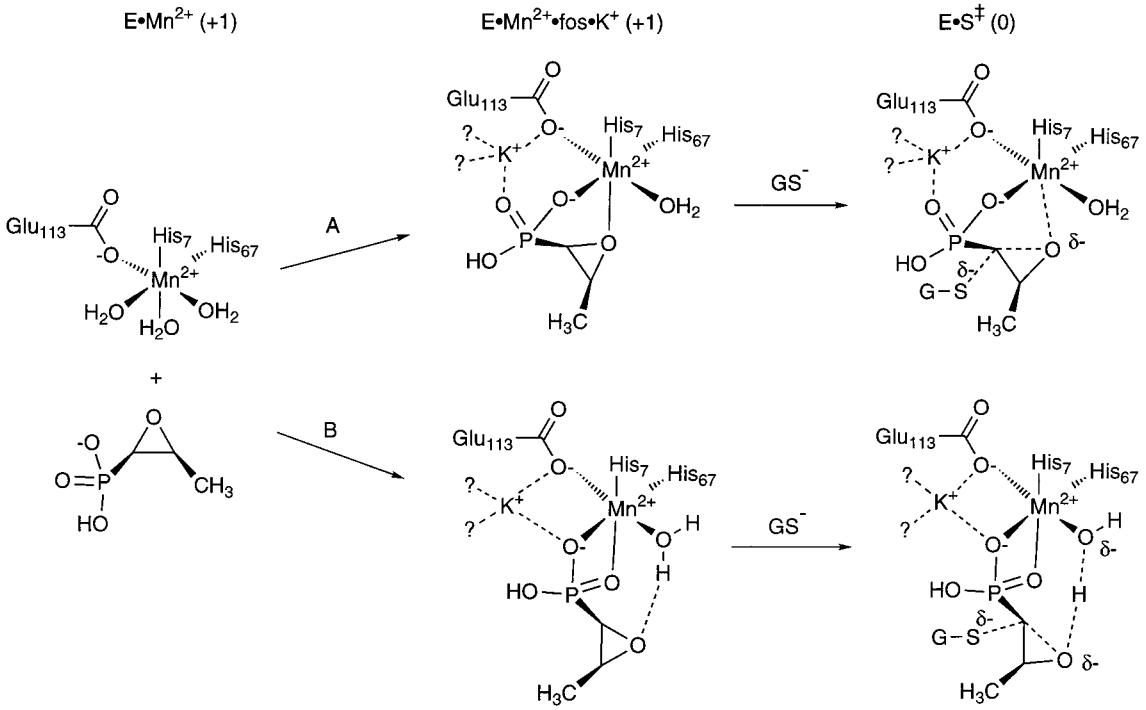

FIGURE 6: Possible roles for K^+ and Mn^{2+} in the FosA-catalyzed addition of GSH to fosfomycin. The net charge at the metal center of each complex is given in parentheses. If fosfomycin is bound as the dianion, then the charges at the metal center for E·Mn^{2+}, E·Mn^{2+}·fos·K^+, and E·S‡ are +1, 0, and −1, respectively. Other coordination geometries not illustrated are also possible including monodentate or tridentate coordination of fosfomycin to the metal.

enzyme along with the absence of an effect of GSH on the spectrum prompted us to suggest previously that fosfomycin binds to the metal center during catalysis (*2*). This involves bringing an additional anion into or near the coordination sphere of the metal for formation of the E·Mn^{2+}·fos complex which is subsequently attacked by the thiolate anion of glutathione. Inasmuch as metal binding sites in proteins tend toward electroneutrality (*21*), the K^+ ion may assist in preserving a neutral or low charge in the active site during catalysis. The net charge in the metal site of E·Mn^{2+} is +1 assuming the ligands to the metal are two neutral imidazole groups, one carboxylate, and three water molecules. Addition of the fosfomycin anion to form the ternary E·Mn^{2+}·fos complex results in a neutral metal site in the absence of K^+ or a charge of +1 in its presence (Figure 6). If fosfomycin were bound as the dianion (not shown), then the net charge would be 0 in the presence of K^+. Whether the K^+ ion actually bridges the carboxylate of E113 and the phosphonate as indicated in Figure 6 is, of course, unknown. However, it is suggested by the fact that both E113 and the substrate must be present to observe the effect of K^+ on the EPR spectrum of the metal.

The proposed transition state for the reaction of GSH with the ternary complex involves approach of a second anion (GS^-) to the metal site. The opening of the oxirane ring would obviously benefit from delocalization of the developing charge on the oxirane oxygen. This could be accomplished in several ways including the metal acting directly as a Lewis acid (as in path A) or through protonation, perhaps by a metal-bound water molecule (path B) as illustrated in Figure 6. In either of these scenarios, the K^+ ion serves to neutralize, indirectly, the developing charge about the metal center in the transition state. The electrophilicity of the metal center is enhanced by the presence of K^+ making it better able to delocalize charge in the transition state either directly (A) or through an intervening water molecule (B).

Even though the structures of the ground and transition states posited in Figure 6 are certainly not correct in every detail, the idea of K^+ enhancing the reactivity of the complex by charge neutralization is attractive. There is also ample precedence for it from the detailed studies of pyruvate kinase. It is not clear if other protein ligands from FosA are involved in binding K^+ as is the case with pyruvate kinase. The K^+ site on pyruvate kinase is composed of four ligands from the protein including the side chains of N74, S76, and D112 and the main-chain carbonyl of T113 and one from the phosphoryl group of the substrate (ATP or PEP) (*22*, *23*). The structures proposed in Figure 6 bear some resemblance to that determined for rabbit muscle pyruvate kinase in that the phosphonyl group of fosfomycin bridges the Mn^{2+} and K^+ ions in much the same way that the γ-phosphoryl group of ATP bridges Mg^{2+} and K^+ in pyruvate kinase (*23*).[4] The functions of the three cations in pyruvate kinase are to screen the repulsive Coulombic interactions arising from the reaction of two anionic species and to enhance the electrophilicity of the phosphorus atom undergoing reaction. This is analogous to the roles for the cations in FosA except the electrophilic center is the carbon adjacent to the phosphonyl group.

The behavior of the E113Q mutant is consistent with the proposition that the K^+ ion helps balance the charge at the metal center, further lowering the activation barrier for addition of the anionic nucleophile. This mutational removal

[4] In the case of pyruvate kinase, there are two Mg^{2+} ions involved in catalysis. One is coordinated to the protein and the γ-phosphoryl group of ATP while the other is coordinated in a tridentate fashion to the α-, β-, and γ-phosphoryl groups of ATP. Thus, all three cations are bridged by the γ-phosphoryl group of ATP.

of the dependence on a monovalent cation is a more subtle variation on the mutational replacement of the K^+ ion in pyruvate kinase (*24*). In a very simple and elegant experiment, Reed and co-workers were able to replace the K^+ ion in pyruvate kinase with an appropriately positioned lysine side chain as in the E117K mutant. Thus, the charge in the active site of the E117K variant is maintained by the placement of an intramolecular cation, namely, the protonated ϵ-amino group, in the K^+ binding site. In contrast, the E113Q mutation in FosA removes the single anion in the ligand field of the divalent cation so there is no longer a need for an additional external cation to balance the charge in the transition state.

CONCLUSIONS

Sequence alignments with related enzymes whose structures are known and the physical, catalytic, and microbiological properties of FosA mutants clearly indicate that the three metal ligands in the divalent cation binding site are the side chains of H7, H67, and E113. Physiologic concentrations of K^+ activate FosA by a factor of 100-fold. Binding of the monovalent cation appears to require the presence of the substrate fosfomycin and the carboxylate of E113. That the K^+ activation is abolished in the E113Q mutant suggests that the monovalent cation is necessary to balance the charge around the divalent metal site for optimum stabilization of the transition state.

ACKNOWLEDGMENT

We thank Prof. George Reed for helpful discussions and the use of the EPR and NMR instrumentation at the Enzyme Institute, University of Wisconsin, Madison, Prof. John Gerlt for the multiple sequence alignment reported in the Supporting Information and for pointing out that methylmalonyl-CoA epimerase is a member of the same superfamily as FosA, and Marcus Voehler for assistance in obtaining the NMR spectra.

SUPPORTING INFORMATION AVAILABLE

Sequence alignment of FosA with other members of the metalloenzyme superfamily and HMBC NMR spectrum of the mixture of product isomers 1 and 2 (2 figures) (5 pages). This material is available free of charge via the Internet at http://pubs.acs.org.

REFERENCES

1. Arca, P., Rico, M., Brana, A. F., Villar, C. J., Hardisson, C., and Suarez, J. E. (1988) *Antimicrob. Agents Chemother. 32*, 1552−1556.
2. Bernat, B. A., Laughlin, L. T., and Armstrong, R. N. (1997) *Biochemistry 36*, 3050−3055.
3. Bernat, B. A., Laughlin, L. T., and Armstrong, R. N. (1998) *J. Org. Chem. 63*, 3378−3380.
4. Armstrong, R. N. (1998) *Curr. Opin. Chem. Biol. 2*, 618−623.
5. Cameron, A. D., Olin, B., Ridderstom, M., Mannervik, B., and Jones, T. A. (1997) *EMBO J. 16*, 3386−3395.
6. Han, S., Eltis, L. D., Tmmis, K. N., Muchmore, S. W., and Bolin, J. T. (1995) *Science 270*, 976−980.
7. Kunkel, T. (1985) *Proc. Natl. Acad. Sci. U.S.A. 82*, 488−492.
8. Segal, I. (1975) *Enzyme Kinetics*, pp 57−59, John Wiley and Sons, Inc., New York.
9. Kayne, F. J. (1971) *Arch. Biochem. Biophys. 143*, 232−239.
10. Kachmar, J. F., and Boyer P. B. (1953) *J. Biol. Chem. 200*, 669−682.
11. Reed, G. H., and Cohn, M. (1973) *J. Biol. Chem. 248*, 6436−6442.
12. Reed, G. H., and Markham, G. D. (1984) *Biol. Magn. Reson. 6*, 73−142.
13. Zilhao, R., and Courvalin, P. (1990) *FEMS Microbiol. Lett. 68*, 267−272.
14. Kunst, F., et al. (1997) *Nature 390*, 249−256.
15. Farrington, G. K., Kumar, A., and Wedler, F. C. (1985) *J. Med. Chem. 28*, 1668−1673.
16. Phillion, D. P., and Andrew, S. S. (1986) *Tetrahedron Lett.*, 1477−1479.
17. Kahan, F. M., Kahan, J. S., Cassidy, P. J., and Kroop, H. (1974) *Ann. N.Y. Acad. Sci. 235*, 364−385.
18. Marquardt, J. L., Brown, E. D., Lane, W. S., Haley, T. M., Ichskawa, Y., Wong, C.-H., & Walsh, C. T. (1994) *Biochemistry 33*, 10646−10651.
19. Skarzynski, T., Mistry, A., Wonacott, A., Huchinson, S. E., Kelly, V. A., and Duncan, K. (1996) *Structure 4*, 1465−1474.
20. Silver, S. (1996) *Transport of Inorganic Cations in Escherichia coli and Salmonella* (Neidhardt, F. C., Ed.) p 1093, ASM Press, Washington, DC.
21. Lippard, S. J., and Berg, J. M. (1994) *Principles of Bioinorganic Chemistry*, pp 218−221, University Science Books, Mill Valley, CA.
22. Larson, T. M., Benning, M. M., Wesenberg, G. E., Rayment, I., and Reed, G. H. (1997) *Arch. Biochem. Biophys. 345*, 199−206.
23. Larson, T. M., Benning, M. M., Rayment, I., and Reed, G. H. (1998) *Biochemistry 37*, 6247−6255.
24. Laughlin, L. T., and Reed, G. H. (1997) *Arch. Biochem. Biophys. 348*, 262−267.

BI990391Y